

# Visualization of Receptor-mediated Endocytosis in Yeast

Jon Mulholland,\* James Konopka,<sup>†</sup> Birgit Singer-Kruger,<sup>‡§</sup> Marino Zerial,<sup>‡</sup> and David Botstein\*<sup>||</sup>

\*Department of Genetics, Stanford University School of Medicine, Stanford, California 94305-5120;

<sup>†</sup>Department of Microbiology, State University of New York, Stony Brook, New York 11794; and

<sup>‡</sup>European Molecular Biology Laboratory, 69117 Heidelberg, Germany

Submitted November 11, 1998; Accepted December 21, 1998

Monitoring Editor: Randy W. Schekman

We studied the ligand-induced endocytosis of the yeast  $\alpha$ -factor receptor Ste2p by immuno-electron microscopy. We observed and quantitated time-dependent loss of Ste2p from the plasma membrane of cells exposed to  $\alpha$ -factor. This ligand-induced internalization of Ste2p was blocked in the well-characterized endocytosis-deficient mutant *sac6* $\Delta$ . We provide evidence that implicates furrow-like invaginations of the plasma membrane as the site of receptor internalization. These invaginations are distinct from the finger-like plasma membrane invaginations within actin cortical patches. Consistent with this, we show that Ste2p is not located within the cortical actin patch before and during receptor-mediated endocytosis. In wild-type cells exposed to  $\alpha$ -factor we also observed and quantitated a time-dependent accumulation of Ste2p in intracellular, membrane-bound compartments. These compartments have a characteristic electron density but variable shape and size and are often located adjacent to the vacuole. In immuno-electron microscopy experiments these compartments labeled with antibodies directed against the rab5 homologue Ypt51p (Vps21p), the resident vacuolar protease carboxypeptidase Y, and the vacuolar H<sup>+</sup>-ATPase Vph1p. Using a new double-labeling technique we have colocalized antibodies against Ste2p and carboxypeptidase Y to this compartment, thereby identifying these compartments as prevacuolar late endosomes.

## INTRODUCTION

Endocytosis is the internalization of plasma membrane-associated proteins and molecules (along with extracellular fluids) via specialized plasma membrane domains (reviewed in Mukherjee *et al.*, 1997). These endocytic domains classically were defined in mammalian cells by clathrin-coated pits (Pearse, 1976) and more recently by non-clathrin-coated plasma membrane invaginations, such as caveolae, as well (Rothberg, *et al.*, 1992). In receptor-mediated endocytosis, exposure to specific ligands induces the clustering of receptor-ligand complexes into these plasma membrane domains (Anderson *et al.*, 1978; Goldstein *et al.*,

1979). From these domains endocytic vesicles are formed and subsequently deliver ligand-receptor complexes to "early" endosomal compartments. From these early endosomes receptors are recycled to the cell surface, whereas ligands destined for degradation continue on to "late" endosomal compartments. The late endosome is a prelysosomal compartment involved in the delivery of both lysosomal enzymes and internalized molecules to lysosomes. Both the early and late endosomal compartments have been isolated biochemically and can be defined at the molecular level by the presence of characteristic Rab GTPases (reviewed in Zerial and Stenmark, 1993).

Receptor-mediated endocytosis in budding yeast (*Saccharomyces cerevisiae*) appears largely analogous to receptor-mediated endocytosis in animal cells (reviewed in Bryant and Stevens, 1998; Geli and Riezman, 1998). Yeast has been shown to carry out ligand-

<sup>§</sup> Present address: Institute für Biochemie, Universität Stuttgart, Stuttgart, Germany.

<sup>||</sup> Corresponding author. E-mail address: botstein@genome.stanford.edu.

induced endocytosis of its mating factors by receptor-mediated mechanisms (Chvatchko *et al.*, 1986; Jenness and Spatrick, 1986; Davis *et al.*, 1993). Immunofluorescence microscopy and cell fractionation studies have shown that Ste2p (the receptor for the yeast mating pheromone  $\alpha$ -factor) is located on the plasma membrane of MATa cells (Schandel and Jenness, 1994; Hicke *et al.*, 1997). Upon exposure to  $\alpha$ -factor, MATa cells internalize bound ligand in a time-, energy-, and temperature-dependent manner (Chvatchko *et al.*, 1986; Jenness and Spatrick, 1986; Dulic and Riezman, 1989). The internalization of  $\alpha$ -factor is coincident with the down-regulation of its receptor, Ste2p (Schandel and Jenness, 1994). However, the receptor apparently is not recycled; both Ste2p and its ligand are degraded within the lysosomal-like vacuole (Singer and Riezman; 1990; Schandel and Jenness, 1994).

In yeast, the actin cytoskeleton appears to play an essential role in the internalization step(s) of endocytosis (reviewed in Botstein *et al.*, 1997; Bryant and Stevens, 1998). Direct testing of many actin cytoskeleton mutants (*act1*, *sac6*, *cof*, *arp2*, and *pan1*) showed them to be blocked at the internalization step of endocytosis (Kubler and Riezman, 1993; Lappalainen and Drubin, 1997; Moreau *et al.*, 1997; Tang *et al.*, 1997). Furthermore, genetic screens designed to identify genes required for internalization of  $\alpha$ -factor have consistently yielded mutations in genes that are expected to interact with the actin cytoskeleton (Raths *et al.*, 1993; Kubler *et al.*, 1994; Munn *et al.*, 1995; Wendland *et al.*, 1996; Givan and Sprague, 1997; Geli and Riezman, 1996). The yeast actin cytoskeleton consists of two major structures, actin cables and cortical actin patches (reviewed in Botstein *et al.*, 1997). At the ultrastructural level the cortical actin patch consists of a finger-like invagination of plasma membrane around which actin and associated actin-binding proteins are organized (Mulholland *et al.*, 1994). This architecture, together with the colocalization of proteins required for endocytosis such as Sla2p (End4p), cofilin, End3p, and Pan1p, made the cortical actin patch an attractive candidate for the site of endocytosis in yeast.

Once internalized,  $\alpha$ -factor is transported, via two kinetically defined and biochemically separable compartments, to the yeast vacuole (Singer and Riezman, 1990; Singer-Kruger *et al.*, 1993). These compartments are associated with yeast homologues (Ypt proteins) of the mammalian Rab proteins (Singer-Kruger *et al.*, 1994). Most recently, studies using antibodies directed against Ste2p have demonstrated that, like its ligand, internalized receptor is transported to the yeast vacuole via two distinct compartments (Hicke *et al.*, 1997). At the resolution of immunofluorescence light microscopy, these compartments resemble in morphology and cellular distribution the early and late endosomal compartments of mammalian cells.

In mammalian cells, a branch of the exocytic pathway converges with the endocytic pathway in a prelysosomal compartment (i.e., the late endosome). Similarly in yeast, enzymes destined for the yeast vacuole are selectively transported as inactive zymogens from a late Golgi compartment to a distinct prevacuole compartment (reviewed in Bryant and Stevens, 1998). In cells exposed to  $\alpha$ -factor, this prevacuole compartment contains both the Golgi-modified, proenzyme form of vacuolar enzymes and endocytosed  $^{35}\text{S}$ - $\alpha$ -factor (Raymond *et al.*, 1992; Vida *et al.*, 1993; Piper *et al.*, 1995; Rieder *et al.*, 1996). Thus, in yeast the biosynthetic and endocytic pathways converge in a prevacuole, endosome-like compartment. Whether this prevacuole compartment corresponds to the kinetically defined early or late endosome has not been determined directly.

Although genetic and biochemical studies have defined much of the machinery and kinetics of receptor-mediated endocytosis and transport, there has been limited success in defining the morphological components of the yeast endocytic pathway. Specifically there has been no direct, immunological identification of endocytic domain(s) on the yeast plasma membrane and only minimal visualization of the internal compartments. More importantly, transport of internalized Ste2p to the yeast vacuole has not been systematically followed at the ultrastructural level. Using immuno-electron microscopy (EM) we have begun to visualize and define the endocytic system of yeast.

## MATERIALS AND METHODS

### *Yeast Strains and Growth Conditions*

The yeast strains used in this study are RH448, MATa *his4-619 leu2 ura3 lys2 bar1-1* (Riezman Laboratory; Biozentrum, Basel Switzerland); DBY6401, MATa *ste2::HIS3 his3 $\Delta$ 200 leu2-3,112 ura3-52 bar1::URA3*; and DBY7214, MATa *sac6::LEU2 his3 $\Delta$ 200 leu2-3,112 ura3-52 lys2-801*. All strains are direct descendant of strain S288C. Strains were grown either at the permissive temperature of 25°C or the nonpermissive temperature of 37°C in yeast extract peptone (YEP) medium (Sherman *et al.*, 1986) containing 2% glucose. Cell cultures were harvested for immuno-EM at a cell density of between 0.4 and 0.6 (OD<sub>600</sub>). All cells were fixed and processed for immuno-EM as described below.

### *Fixation and Processing for Immuno-EM*

Cells were fixed and processed as described by Mulholland *et al.* (1994). One hundred-milliliter cultures of exponentially growing cells ( $5 \times 10^6$  cells/ml) in YEP-2% glucose medium were quickly harvested by vacuum filtration over a 0.45- $\mu\text{m}$  nitrocellulose membrane; filtration was stopped when the total volume in the filter apparatus was ~5 ml. To this concentrated cell suspension, still on the filter membrane, 25 ml of freshly prepared, room temperature fixative (40 mM potassium phosphate, pH 6.7, 0.8 M sorbitol, 4% formaldehyde freshly prepared from paraformaldehyde [Polysciences, Warrington, PA], 0.4% glutaraldehyde [EM grade, Polysciences], 1 mM MgCl<sub>2</sub>, and 1 mM EGTA, pH 8) was added and mixed rapidly with the cells by pipetting the suspension several times. The cell suspension was then transferred to a 50-ml polypropylene centrifuge tube and incubated at room temperature for 1 h.

The fixed cells were then centrifuged at low speed in a clinical centrifuge, and the pellet was resuspended in 25 ml of 40 mM potassium phosphate buffer (pH 6.7) containing 0.50 M sorbitol. The cells were again centrifuged and washed in 40 mM potassium phosphate buffer (pH 6.7) containing 0.25 M sorbitol. A final wash in 5 ml of 40 mM potassium phosphate buffer (pH 6.7) was performed, and the fixed cells were transferred to a glass (13 × 100-mm) test tube. As described previously (van Tuinen and Riezman, 1987) the final pellet of fixed cells was resuspended in 5 ml of 1% sodium metaperiodate, incubated for 10 min at room temperature, and then centrifuged and resuspended in 5 ml of distilled water. Next the cells were centrifuged, resuspended in 5 ml of 50 mM ammonium chloride, and incubated for 10 min at room temperature.

Before dehydration, the cells were washed once in distilled water, centrifuged at low speed, and then dehydrated (on ice) by resuspending the cell pellet in 30% (vol/vol) ice-cold ethanol and incubating on ice for 5 min. The cells were similarly centrifuged and sequentially resuspended in 50, 70, 80, 85, 90, and 95% ice-cold ethanol and finally once in 100% ice-cold ethanol. A final dehydration and centrifugation in 100% ethanol at room temperature was performed twice. The dehydrated cells then were infiltrated with room temperature L.R. White resin (Polysciences) and prepared for polymerization as described by Wright and Rine (1989), except that infiltration of resin into the cells was done without application of vacuum, and harvesting of cells was by centrifugation. The resin was polymerized by incubation at 47°C for ~48 h.

Thin sections measuring ~60–70 nm (as determined by a gray-silver interference color) were cut with a diamond knife and were picked up on 300 mesh nickel grids (Polysciences), which had been made sticky with a dilute Formvar solution (Wright and Rine, 1989).

### Antibody Production, Immunolabeling, and EM

Affinity-purified antibodies directed against Ste2p were generated as follows. Anti-Ste2p antiserum was raised in rabbits injected with a trpE-Ste2p fusion protein that contained the 100 N-terminal residues of Ste2p (Konopka *et al.*, 1988); 7.5 ml of this antiserum was adsorbed against *ste2Δ* whole-cell extract that had been run on four SDS-PAGE gels and transferred to nitrocellulose. The Ste2p antiserum was sequentially adsorbed to those four nitrocellulose blots. Adsorbed antiserum was then affinity purified on a GST-Ste2p column that was prepared using a GST fusion protein containing the 45 N-terminal residues of Ste2p that had been overproduced in *Escherichia coli*. Adsorbed anti-Ste2p antiserum was bound to the GST-Ste2p column and then eluted with a low-pH elution (glycine buffer, pH 2.2). Because this preadsorbed, affinity-purified material did not give a completely background-free signal when used at high concentrations in immunofluorescence light microscopy experiments (Konopka, personal observation), it was adsorbed to fixed *ste2Δ* cells. Five sequential adsorptions against  $\sim 2 \times 10^8$  *ste2Δ* cells (formaldehyde fixed and glucuronidase digested) per adsorption were performed. Because this affinity-purified, adsorbed antibody was now too dilute to use conveniently for immunostaining, it was concentrated by ~50-fold in an Amicon (Danvers, MA) Centricon 100 filter. This affinity-purified, adsorbed, and concentrated anti-Ste2p antibody preparation was observed to give strong, specific staining in immunofluorescence (Konopka, personal observation) and immuno-EM experiments.

Production, purification, and characterization of affinity-purified, polyclonal rabbit antibodies to actin, cofilin, carboxypeptidase Y (CPY), Vph1p, and Ypt51p have been described previously (Drubin *et al.*, 1988; Moon *et al.*, 1993; Manolson *et al.*, 1992; Singer-Kruger *et al.*, 1995, respectively). Antibody incubations were performed as described previously by Mulholland *et al.* (1994). All antibodies were diluted in PBST (140 mM NaCl, 3 mM KCl, 8 mM Na<sub>2</sub>HPO<sub>4</sub>, 1.5 mM KH<sub>2</sub>PO<sub>4</sub>, and 0.05% Tween 20) containing 0.5% BSA and 0.5% ovalbumin (Sigma, St. Louis, MO) and were incubated with cell sections mounted on grids as described above. Anti-actin antibodies, anti-cofilin antibodies, anti-Ypt51p antibodies, and anti-

Vph1p antibodies were diluted 1:30; anti-CPY antibodies were diluted 1:5; and anti-Ste2p antibodies were diluted 1:15. It should be noted that some localization of anti-Ypt51p to the vacuole was observed. However, this vacuolar localization was also observed in *Ypt51Δ* cells and was thus assumed to be nonspecific.

The 10-nm gold-conjugated, anti-rabbit IgG (goat) secondary antibodies (BioCell, Cardiff, United Kingdom) were all diluted 1:50 in PBST, 0.5% BSA, and 0.5% ovalbumin. In the absence of the primary antibody, the anti-rabbit secondary antibodies did not react with the cell sections. After immunolocalization cell sections were postfixed and stained with uranyl acetate and lead citrate as previously described (Mulholland *et al.*, 1994). All observations were made on a vintage Philips (Mahwah, NJ) 300 electron microscope at an accelerating voltage of 80 kV using a 20- $\mu$ m-diameter objective aperture.

### Double-Label Immuno-EM

The first double-label technique uses a conventional blocking step to prevent the first antibody-immunogold complex from reacting with second antibody-immunogold complex (van Genderen *et al.*, 1991). The primary antibody (anti-Ste2p) and gold-labeled secondary antibody were applied as described above. Then the cell sections were briefly washed in PBST and incubated in 4% formaldehyde, 0.1% glutaraldehyde, and 40 mM potassium phosphate (pH 6.7) for 15 min at room temperature to block further secondary antibody adsorption. The immunolocalized, blocked cell sections were then washed five times (5 min each time) in 50  $\mu$ l of PBST. Last, the cell sections were incubated with anti-cofilin antibodies followed by anti-rabbit (IgG) 15-nm gold secondary antibodies and postfixed and stained with uranyl acetate and lead citrate as described above. This immuno-EM procedure greatly reduced 15-nm gold particle localization to the first antibody-anti-Ste2p complex, as determined by a lack of colocalization of anti-Ste2p 10-nm immunogold and 15-nm gold particles in prevacuole membrane-bound compartments where cofilin is not located. This blocking step only slightly reduced the immunoreactivity of cofilin itself. However, it should be noted that this worked only for the cofilin antibodies as the second stain. The immunoreactivity of the epitopes recognized by the other antibodies appeared to be eliminated by the blocking procedure.

In the second double-localization method, which we call "adjacent-face double localization," two immediately sequential sections (80–100 nm thick) were picked up on two separate 200 mesh nickel grids (Polysciences). These sections were cut to be almost large enough to cover the entire 3.05-mm grid. Each section was then subjected to the standard (single), immunogold localization as described above, each with a different primary antibody. Only one side of each of the sections was exposed to antibody. The side that was exposed to antibody on each of the two sections was the side or "face" that was contiguous with the other section before sectioning. To accomplish this, the first section was picked up by touching the grid to the section from above; the second section was picked up by submerging the grid in the water of the sectioning knife and picking the section up from below. These two different ways of picking up the sequential sections allowed the adjacent face of both sections to be comparably exposed to subsequent antibody incubations and staining procedures. To minimize possible differences in detection of the primary antibody, the same 10-nm (anti-rabbit) gold secondary antibody was used on both immunolocalized sections. The immunogold localized section pairs were then stained with uranyl acetate and lead citrate as described above.

Each of the adjacent-face double-localization sections was examined in our Philips 300 electron microscope equipped with a custom-installed 1 kilobit Bioscan CCD camera (Gatan, Pleasanton, CA). Using low-magnification images, areas of the adjacent-face pair that were visible on both grids were identified and marked, allowing us subsequently to find coordinate areas and matching individual cell sections on each of the adjacent-face sections. We

then separately acquired high-magnification digital images of cell sections having localization to proteins A and B. The digital image pairs were merged using Photoshop software (Adobe Systems, San Jose, CA) and examined for colocalization of anti-A and anti-B antibodies. It should be noted that this technique may eliminate considerable observer bias, because the colocalization is not evident until the merging step.

In our figures, we show each of the primary images with minimal processing (only contrast and brightness were adjusted). The merged images were processed more extensively to emphasize localization results; the 10-nm immunogold particles were colorized and, for ease of visualization, enlarged.

The following comments should be kept in mind when examining the localization results presented here. In our immuno-EM techniques, immunolocalization occurs after the cells have been chemically fixed, dehydrated, embedded in resin, and sectioned. Therefore, although structures can be visualized throughout the cell section, only antigens that are within the first 5 nm of either side of the cell section surface are accessible to antibody. Therefore, in the adjacent-face double-localization technique, colocalization of two proteins will be restricted to an area of ~10 nm (~5 nm on each section) sandwiched between two cell sections. Thus, it is possible to observe localization of an antigen on a cell section in which there is no visible structure only to find the structure clearly visible in the sequential section. This result suggests that in the first section the structure was just "grazed" during sectioning; proteins are present on the surface of the section, but not enough of the structure is present to visualize. Conversely, it is possible to observe a structure that in previous experiments had localized a specific antibody, which now shows no localization of that antibody. In this case, observation of the adjacent section shows no structure, suggesting that the structure in the first section was not exposed at the surface of the adjacent face and instead extended in the opposite direction. Thus, in the adjacent-face double-localization technique we expect that, occasionally, colocalization will not be observed for the trivial reason that the structure and or antigen is not present within the narrow 10-nm area of the adjacent faces. Conversely, when colocalization does occur, we are able to infer that the antigens are within  $\leq 10$  nm of each other.

### ***$\alpha$ -Factor Treatment***

Wild-type (RH448), and *sac6* $\Delta$  cell cultures were grown at 25°C in YPD (2%) media to an OD<sub>600</sub> of ~0.4–0.6, and then  $\alpha$ -factor was added to a final concentration of 2.5  $\mu$ M. Wild-type 37°C samples were shifted from 25 to 37°C and preincubated at this temperature for 15 min before the addition of  $\alpha$ -factor. Samples were then taken at 0 min (immediately before addition of  $\alpha$ -factor) and then 5, 10, and 15 min after the addition of  $\alpha$ -factor. These samples were fixed and processed for immuno-EM as described above.

It should be noted that cycloheximide was not used in our internalization assays. Although it is expected under assay conditions that do not block new protein synthesis that there should be a continuous delivery of Ste2p to the plasma membrane, it is also expected that under conditions used in our assay (continuous exposure to high concentrations of  $\alpha$ -factor), newly synthesized  $\alpha$ -factor will be internalized as soon as it reaches the cell surface. Additionally, it has been shown that exposure to  $\alpha$ -factor stimulates *STE2* expression, and the resulting increased production of Ste2p is necessary to observe significant reaccumulation of Ste2p at the plasma membrane. Importantly this reaccumulation of Ste2p does not begin until ~30 min after exposure to  $\alpha$ -factor and does not reach pre- $\alpha$ -factor exposure levels for another 40–50 min (Jenness and Spatrick, 1986). More importantly, Hicke *et al.* (1997) observed an apparent delay in the transport of internalized Ste2p to the vacuole, as well as an apparent accumulation of Ste2p-containing perivacuole compartments, in cells exposed to cycloheximide.

### ***Quantitation of Ste2p Cell Surface Distribution and Internalization***

Loss of Ste2p from the cell surface was quantitated by counting the number of anti-Ste2p antibody localizations (i.e., number of gold particles) at the cell surface of cells taken at  $t = 0, 5, 10,$  and 15 min after exposure to  $\alpha$ -factor. This was done with wild-type cells incubated with  $\alpha$ -factor at 25 and 37°C and with *sac6* $\Delta$  cells incubated with  $\alpha$ -factor at 25°C. The 37°C cultures were preincubated for 15 min at 37°C before exposure to  $\alpha$ -factor. A total of 50 random cell sections were counted for each strain at each of the four time points. The total number of cell surface-associated gold particles (all 50 cell sections) at each time point was then plotted. To control for background labeling, *ste2* $\Delta$  cell sections were localized with anti-Ste2p antibodies, and the numbers of cell surface-associated gold particles were counted on 50 random cell sections. This was done in six independent experiments, giving an average number of cell surface-associated background localizations of 200 particles per 50 cell sections. There was essentially no anti-Ste2p antibody localization to intracellular, endosome-like compartments observed in the *ste2* $\Delta$  cells (3 gold particles localized per ~110 endosome-like compartments observed in 300 cell sections). This data set was also used to quantitate the distribution of anti-Ste2p immunogold over invaginated and noninvaginated areas of the plasma membrane.

## **RESULTS**

### ***Quantitation of Ligand-induced Internalization of Ste2p in Wild Type and an Endocytosis-defective Mutant***

Ste2p, the receptor for yeast  $\alpha$ -factor, is located at the plasma membrane, as determined from subcellular fractionation studies (Schandel and Jenness, 1994). It appears in a spotty distribution over the yeast cell surface when observed by immunofluorescence microscopy (Jackson *et al.*, 1991; Hicke *et al.*, 1997). Upon exposure to  $\alpha$ -factor, wild-type *MATa* cells internalize Ste2p with a half-time of ~8 min (Schandel and Jenness, 1994). The actin cytoskeleton mutant *sac6* $\Delta$  exhibits a lethal phenotype at high temperature (Adams *et al.*, 1991) but is completely defective for internalization of  $\alpha$ -factor at all temperatures (Kubler and Riezman, 1993).

We used immuno-EM techniques to localize Ste2p on the plasma membrane in wild-type cells at a higher level of resolution. Wild-type (RH448) samples were removed from a culture growing at 25°C and immediately fixed and processed for immunogold EM. When applied to wild-type cells, the affinity-purified anti-Ste2p antibodies unevenly labeled the cell surface (Figure 1). We observed substantial clusters of gold particles on invaginations of the plasma membrane (Figure 1, C–E, arrows). The clustering of Ste2p in these invaginations is entirely consistent with the spotty staining pattern previously observed using immunofluorescence light microscopy (Hicke *et al.*, 1997).

We quantitated, by counting gold particles, Ste2p cell surface localization and followed its ligand-induced internalization in wild-type and *sac6* $\Delta$  cells exposed to  $\alpha$ -factor in samples taken at 0, 5, 10, and 15

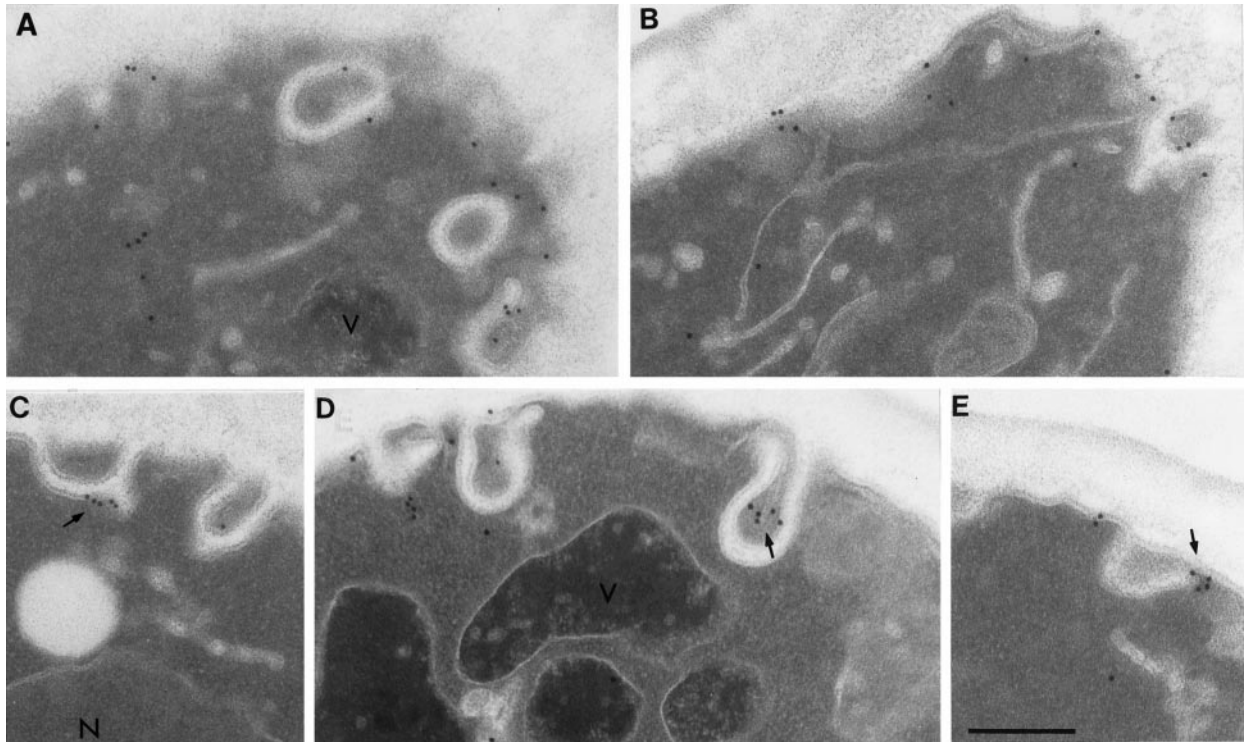


**Figure 1.** Anti-Ste2p antibodies localize to the cell surface and plasma membrane invaginations of wild-type cells (RH448) grown at 25°C. Note the clustered localization of Ste2p to the invaginations (arrows) in C–E. N, nucleus; V, vacuole. Bar, 0.5  $\mu$ m.

min after exposure to  $\alpha$ -factor. This was done with wild-type cells incubated with  $\alpha$ -factor at 25 and 37°C and with *sac6* $\Delta$  cells incubated with  $\alpha$ -factor at 25°C. A total of 50 random cell sections were counted for each strain at each of the four time points. To control for background labeling, *ste2* $\Delta$  cell sections were incubated with anti-Ste2p antibodies, and the numbers of cell surface-associated gold particles were again counted on 50 random cell sections. This was done in six independent experiments, giving an average of 200 gold particles per 50 cell sections. This number was significantly less than that observed in *STE2*<sup>+</sup> strains before addition of  $\alpha$ -factor.

As can be seen in Figure 2, wild-type cells internalized Ste2p to background levels within 15 min of exposure to  $\alpha$ -factor at both 25 and 37°C. In contrast, and as expected, the *sac6* $\Delta$  strain, growing at 25°C, failed completely to internalize Ste2p. Together these results demonstrate that we are observing  $\alpha$ -factor-induced internalization of Ste2p.

#### Localization of Internalized Ste2p

After 5 min of exposure to  $\alpha$ -factor, 50% of the cell surface-associated Ste2p had been internalized (Figure 2). Whereas we found little localization of Ste2p inside cells at the beginning of the experiment ( $t = 0$

min; see Figure 1), at 5 min after ligand addition we found abundant intracellular Ste2p immunogold localization on small (~20–30 nm) vesicles that often were located next to invaginations of the plasma membrane as well as next to tubular-vesicular membrane structures (Figure 3, A and B). Occasionally we observed that some of the anti-Ste2p-positive, tubular-vesicular structures were associated with enlarged tubules that had an internal morphology suggestive of membranes (Figure 3D). Intracellular localization of anti-Ste2p antibodies to the small vesicles and tubular-vesicular structures was not evident before ligand-induced endocytosis.

After 10 min of exposure to  $\alpha$ -factor the cell surface-associated localization of Ste2p antibodies was near background levels at both 25 and 37°C (Figure 1). Examination of cell sections taken from samples exposed to  $\alpha$ -factor for 10 and 15 min revealed prominent anti-Ste2p antibody localization to membrane-bound compartments that were different in morphology than the majority of those observed just after exposure to  $\alpha$ -factor. These compartments had a characteristic electron density and often appeared to contain internal membranes (Figure 3, E–H). Interestingly, they had variable shapes and sizes ranging from round and oval to “peanut” and between 100 and 300 nm across and were often clustered

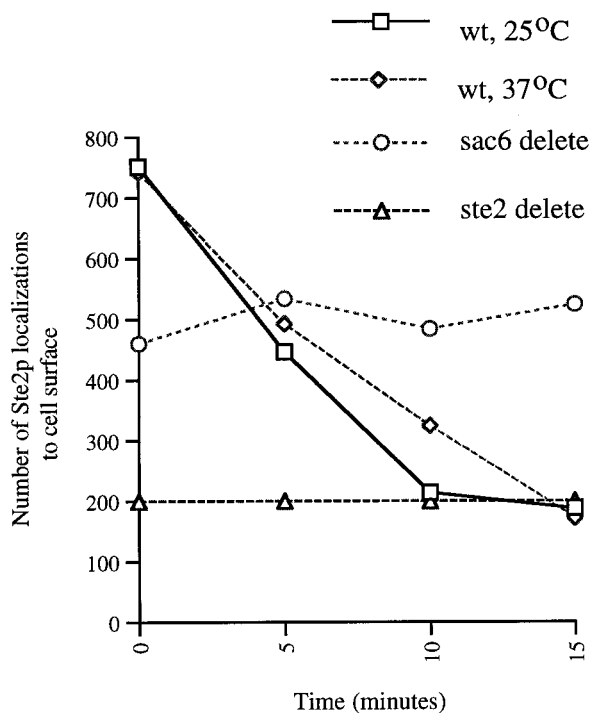


**Figure 2.** Ste2p localization is quantitatively lost, in a time- and  $\alpha$ -factor-dependent manner from the cell surface of wild-type cells at 25 and 37°C. In the endocytosis mutant, *sac6* $\Delta$  Ste2p remains localized to the cell surface after exposure to  $\alpha$ -factor at 25°C. To indicate nonspecific background, the average number of anti-Ste2p antibody localization to the cell surface of *ste2* $\Delta$  cells grown at 25°C is shown.

adjacent to the vacuole. In serial sections these compartments had an appearance consistent with the idea that they might be fusing with each other as well as with the vacuole (Figure 3, E and F; also see Figure 8). Interestingly, at 37°C (Figure 3, G and H) we observed an extraordinary accumulation of such compartments near the vacuole.

### *Ste2p Is Not Located within the Cortical Actin Patch*

Previous studies have strongly suggested a role for the actin cytoskeleton in the internalization step(s) of receptor-mediated endocytosis. The best-characterized actin-containing structure in yeast is the actin cortical patch. At the ultrastructural level, this structure consists of a finger-like invagination of plasma membrane around which the actin cytoskeleton is organized (Mulholland *et al.*, 1994). Interestingly, many of the internalization-defective mutants have been shown to be defective in proteins that *in vivo* localize to the cortical actin patch (reviewed in Botstein *et al.*, 1997; Bryant and Stevens, 1998). Together these results suggested a role for the cortical actin patch in the inter-

nalization step(s) of endocytosis. To test this hypothesis directly, we used two different double-localization techniques using anti-Ste2p antibodies together with affinity-purified anti-cofilin and anti-actin antibodies.

In the first double-label experiment we used antibodies directed against Ste2p and cofilin. In both immunofluorescence light microscopy (Moon *et al.*, 1993) and immuno-EM experiments (Mulholland *et al.*, 1994), cofilin has been shown to localize to cortical actin patches and not to the actin cables. Therefore, immunogold localization of cofilin can be used to identify the cortical actin patches. Because both the anti-Ste2p and anti-cofilin antibodies used in our experiments were raised in rabbits, their use in double-label experiments produced a problem of the first antibody-immunogold complex (anti-Ste2p-10-nm gold) being “seen” by the antibodies used for the second immunogold localization (anti-cofilin-20-nm gold). To overcome this problem we used the first double-localization procedure described in MATERIALS AND METHODS. In brief, first Ste2p was immunolocalized, using 10-nm gold, to cell sections; after blocking, cofilin was immunolocalized, using 15-nm gold. The double-label procedure was done on cell sections cut from wild-type samples taken just before ( $t = 0$  min) and just after ( $t = 5$  min) exposure to  $\alpha$ -factor. To control for nonspecific localization of our anti-Ste2p antibodies to cortical actin patches, we performed the same double-label experiment described above using cell sections taken from a *ste2* $\Delta$  sample that had not been exposed to  $\alpha$ -factor.

These double-labeled sections were then observed in the electron microscope, and the number of colocalizations of Ste2p and cortical actin patches was counted. A cortical actin patch was defined as a cluster of 10 or more anti-cofilin 15-nm gold particles located over an area of  $\sim 100$ –150 nm. If a membrane was present within a cluster of anti-cofilin gold particles, then five or more gold particles defined a cortical actin patch. Typical localization results are shown in Figure 4, A–C. We examined at least 62 actin patches at each time point and observed similar percentages of 10-nm gold (Ste2p)-positive, cofilin-defined cortical actin patches in wild-type cell sections at  $t = 0$  min (15%) and  $t = 5$  min (14%), as in the *ste2* $\Delta$  control cell sections (17%). Thus, surprisingly, we found no evidence for Ste2p in the cortical patches by this method.

To explore further the connection between the cortical actin patch and receptor-mediated endocytosis, we attempted double-label experiments with affinity-purified antibodies directed against Ste2p and actin itself. However, both actin and Ste2p showed a much decreased reactivity with antibodies after the weak fixation step we had previously used to block antibody cross-reactivity. Therefore, we devised the second immuno-EM, double-label technique (adjacent-face double labeling) described in detail in MATERIALS AND METHODS. Two sequen-

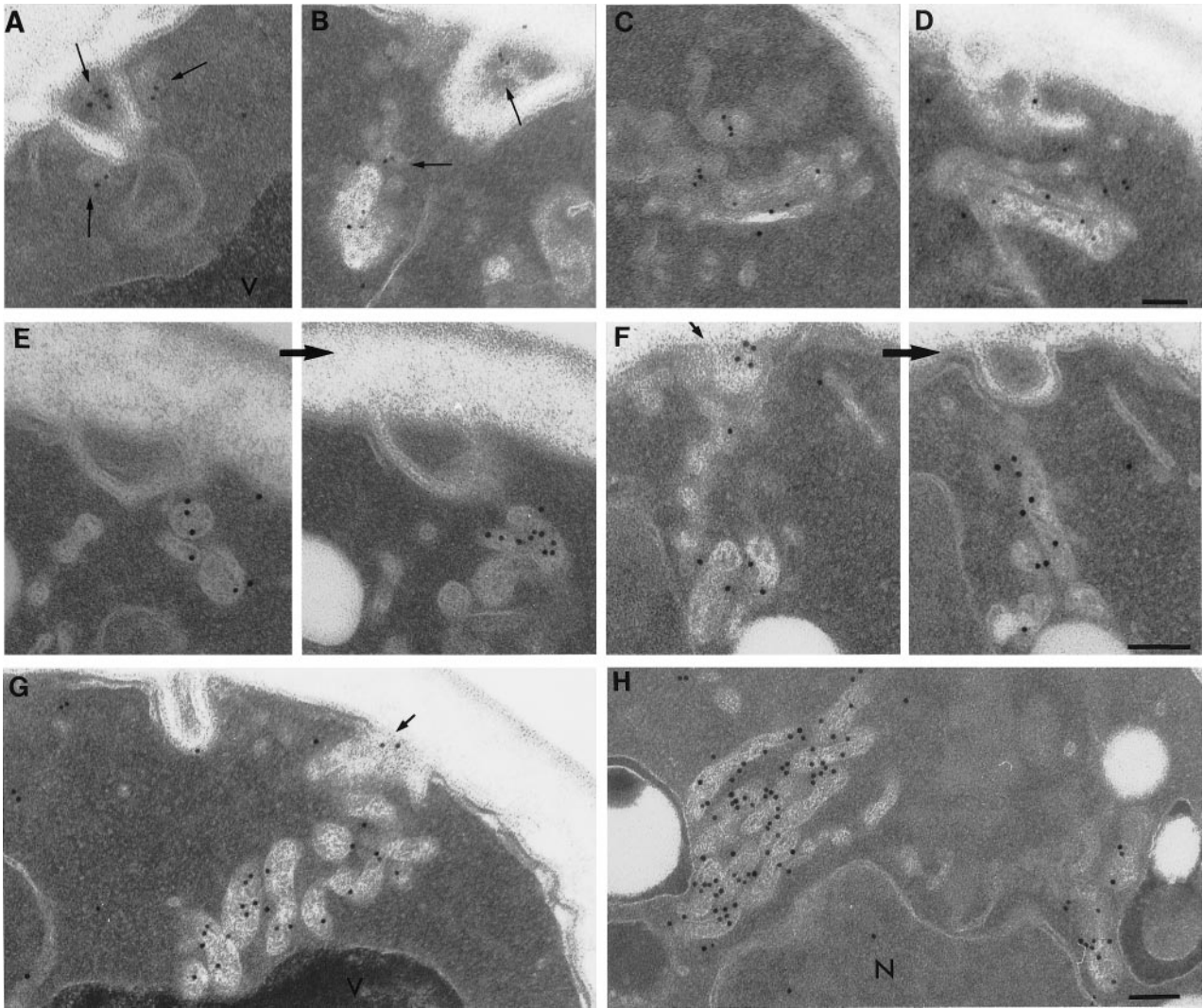


**Figure 3.** After exposure to  $\alpha$ -factor, Ste2p is located in membrane-bound compartments. Wild-type cells (RH448) were taken after 5 min (A–D), 10 min (E), and 15 min (F–H) of continuous exposure to  $\alpha$ -factor. Note small peripheral vesicles (long arrows) and tubular-vesicular compartments to which anti-Ste2p antibodies localize soon after exposure of  $\alpha$ -factor (A–D). Note also the perivacuole compartments that localize antibodies directed against Ste2p (F–H). Many of these compartments appear to contain internal membranes and in sequential sections appear as interconnected tubular-vesicular structures (E and F). After 15 min of exposure to  $\alpha$ -factor at 37°C, perivacuolar compartments accumulate (G and H). Note in F and G the localization of anti-Ste2p antibodies to tangentially cut invaginations of plasma membrane (F and G, short arrows) as well as to the membrane-bound compartments located proximal to these invaginations. V, vacuole; N, nucleus. Bars, 0.5  $\mu$ m.

tial sections are picked up individually on different grids. Each grid is then subjected to a standard (single) immunogold localization with the exception that only one side of the section is exposed to antibody. The side that is exposed to antibody on each of the two sections is the side or face that was contiguous with the other section before sectioning. In this way, the adjacent face of one section was exposed to anti-actin antibodies, and the adjacent face of the other section was exposed to anti-Ste2p antibodies. To minimize differences in antigen de-

tection, the same 10-nm (anti-rabbit) gold secondary antibody was used in both immunogold localizations.

In this experiment the cortical actin patch was defined as an electron-dense patch (~150 nm across) containing an electron-translucent core that was bound by plasma membrane (Mulholland *et al.*, 1994) and to which anti-actin 10-nm gold particles were localized. The pairs were then examined for colocalization of anti-actin-positive cortical actin patches and anti-Ste2p 10-nm gold. This was done for sections cut

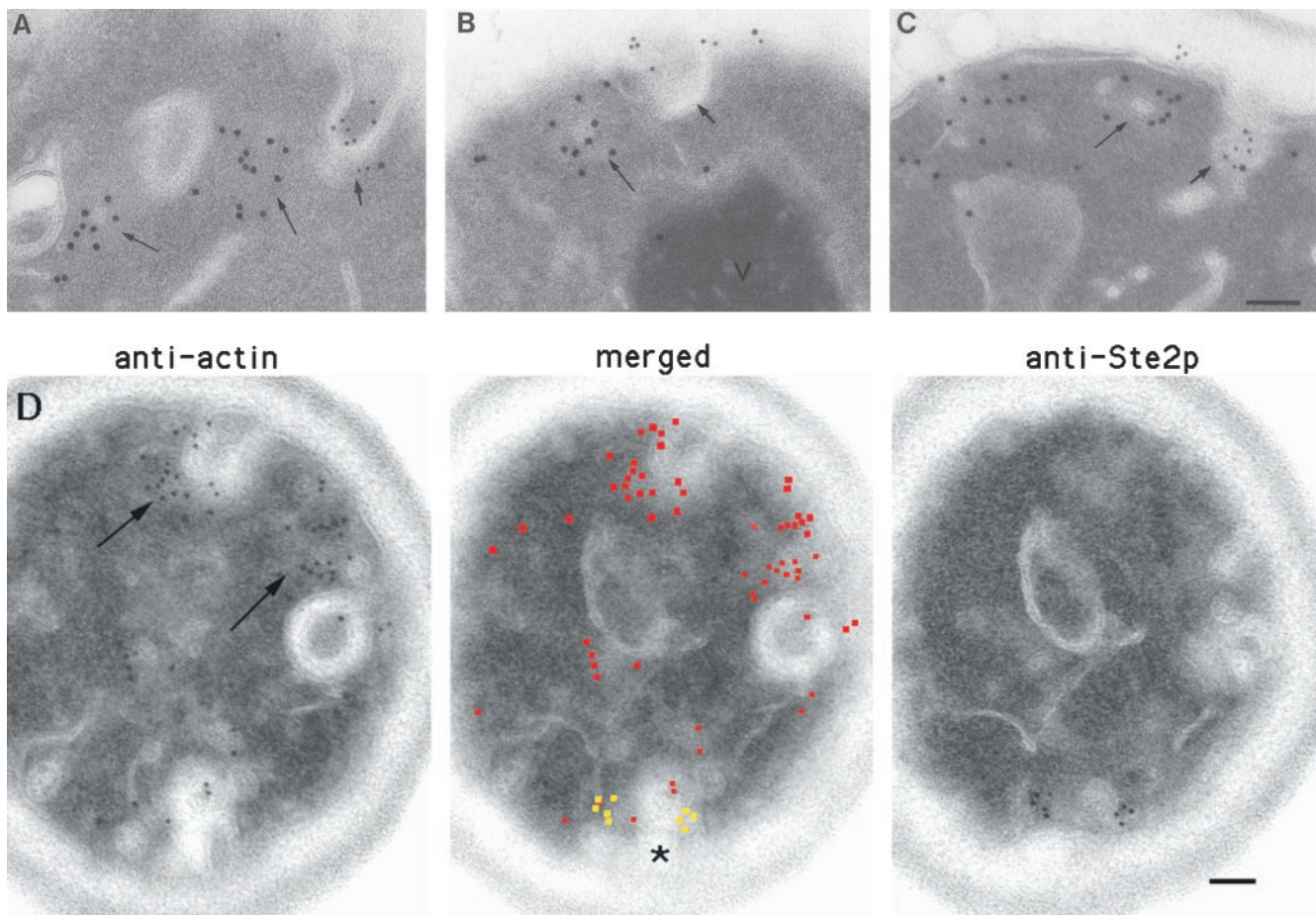


**Figure 4.** Ste2p is not located within the cortical actin patch before (A and B) or after ( $t = 5$  min; C and D) exposure to  $\alpha$ -factor. (A–C) Examples of double labeling with antibodies against cofilin (15-nm gold particles) and Ste2p (10-nm gold particles) on wild-type cells. Note that Ste2p is not observed in the cortical actin patch (long arrows) but is located in furrow-like invaginations of the plasma membrane (short arrows). (D) Example of adjacent-face double localization using anti-actin (red in merged image) and anti-Ste2p (yellow in merged image) antibodies. The asterisk in D indicates a furrow-like invagination that localizes both anti-Ste2p and anti-actin antibodies; long arrows indicate cortical actin patches (see text). Note that the section in D with anti-Ste2p localization does not appear to be associated with an invagination until the adjacent section is examined. Note also that some furrow-like invaginations are located next to actin patches (A, B, and D). Bars, 0.1  $\mu$ m.

from wild-type samples taken just before ( $t = 0$  min) and just after ( $t = 5$  min) exposure to  $\alpha$ -factor at 25°C. A typical anti-Ste2p, anti-actin adjacent-face double localization result is shown in Figure 4D.

We examined double-localization data from 30 cell sections, containing a total of 52 cortical actin patches, at  $t = 0$  min and 33 cell sections, containing a total of 60 cortical actin patches, at  $t = 5$  min after exposure to  $\alpha$ -factor. In both cases, we observed only one cortical actin patch that stained with both antibodies; in each case of apparent colocalization only a single 10-nm gold particle was observed. This level is entirely consistent with background, and thus again we failed to find Ste2p in the cortical patches.

From these two different double-labeling techniques, using two different cortical actin markers, we conclude that Ste2p is not located within the cortical

actin patch before or during  $\alpha$ -factor-induced endocytosis. Furthermore, these results demonstrate that the Ste2p-containing plasma membrane invaginations are not part of the cortical actin patch. However, we did observe occasional cortical actin patches that were located next to plasma membrane invaginations that contained Ste2p (Figure 4). This observation raises the possibility that cortical actin patches associate with Ste2p-containing invaginations in a transient (i.e., short-lived) manner.

#### *Furrow-like Invaginations of the Plasma Membrane Are Implicated in the Internalization of Ste2p*

Two general types of plasma membrane invaginations have been described in yeast: finger-like invaginations that are components of the cortical actin patches and

furrow-like invaginations that show relatively little actin localization (Mulholland *et al.*, 1994). Previous studies had suggested a role for the apparently de novo formation of furrow-like plasma membrane invaginations in pheromone response (Nakagawa *et al.*, 1983); such invaginations have also been implicated in endocytosis in yeast (Wendland *et al.*, 1996; Singer-Kruger *et al.*, 1998).

On sections of wild-type cells we commonly observed anti-Ste2p antibodies localized to the furrow class of invaginations of the plasma membrane, and often the Ste2p localization was noticeably clustered (see Figures 1 and 4 for examples). The furrow-like invaginations often appeared to curl back toward, and in some cases even to fuse, with themselves or the cell surface. Sections through these curled furrows often produced a ring and horseshoe-shaped cisternae that appeared not to be connected to the cell surface. However, serial section analysis shows that these horseshoe membranes are generally continuous on the cell surface (see Figure 6D; Nakagawa *et al.*, 1983). In wild-type cells exposed to  $\alpha$ -factor, we observed clusters of Ste2p localization on many, but not all, of these furrows as well as in endocytic structures (see above) located inside the cells proximal to the invaginations.

To determine whether Ste2p was differentially located in these furrow-like invaginations during ligand-induced endocytosis, we quantitated the appearance of gold particles on the noninvaginated and invaginated areas of the cell surface in wild-type and *sac6* $\Delta$  cells exposed to  $\alpha$ -factor (see MATERIALS AND METHODS). To calibrate any result, we needed some expectation of what a random distribution might look like. We reasoned that the expected random distribution of any marker should be similar to that exhibited by the nonspecific localization of anti-Ste2p immunogold particles over the surface of our *ste2* $\Delta$  strain. Therefore, we first determined the relative distribution of anti-Ste2p gold particles on the surface of a *ste2* $\Delta$  strain, which revealed that  $\sim 67\%$  of all anti-Ste2p cell surface localizations were to the noninvaginated areas, and the remaining  $33 \pm 2.4\%$  were to invaginated areas.

The analysis of the distribution of Ste2p on wild-type and *sac6* cells was done on the same images used to follow loss of Ste2p from the cell surface (see Figure 1 and MATERIALS AND METHODS). Thus, we determined the relative distribution of anti-Ste2p on the cell surface of 50 random cell sections taken just before ( $t = 0$  min) and 5, 10, and 15 min after exposure to  $\alpha$ -factor at both 25 and 37°C for wild type and at 25°C for the *sac6* $\Delta$  strain.

Interestingly, we did not find the expected random distribution of anti-Ste2p gold particles over the plasma membrane of wild-type cells. In wild-type cells, we observed that just before ( $t = 0$  min) incubation in  $\alpha$ -factor at 25°C, there was 15% more anti-Ste2p

gold particles associated with the invaginations of the cell surface then observed in the *ste2* $\Delta$  strain. After ligand-induced internalization, the percentage of Ste2p associated with these invaginations remained significantly above the expected random levels; by 15 min all the Ste2p had been internalized (see Figure 2). Interestingly, before addition of  $\alpha$ -factor at 37°C ( $t = 0$  min), we observed a lower percentage of Ste2p in the invaginations compared with wild-type cells at 25°C. However, after exposure to ligand at 37°C, the percentage of Ste2p localized to invaginations increased to essentially the same level observed in the 25°C samples. This observation may explain why at 37°C compared with 25°C there is a slight increase in the internalization time for receptor (Figure 1). These results indicate that Ste2p is nonrandomly distributed over the yeast cell surface and is somewhat concentrated in invagination of the plasma membrane.

In the *sac6* $\Delta$  cells not exposed to  $\alpha$ -factor ( $t = 0$  min), we observed only a 3% increase above the expected random level of anti-Ste2p localization to plasma membrane invaginations. We suspect that this represents a random distribution over the surface of our *sac6* $\Delta$  strain; significantly, the distribution of Ste2p over the cell surface of *sac6* $\Delta$  cells remained relatively unchanged after exposure to  $\alpha$ -factor (Figure 5). Thus, in this actin cytoskeleton mutant it appears that Ste2p is not differentially located in invaginations of the plasma membrane, and this distribution does not change after exposure to ligand. It should be noted that the average number of plasma membrane invaginations in wild-type and *sac6* $\Delta$  cells did not change after exposure to  $\alpha$ -factor.

Although we have shown (see above) that Ste2p is not located within the cortical actin patch during endocytosis, it is still expected that the actin cytoskeleton will be present at the site of Ste2p internalization. Therefore, to determine whether the Ste2p-containing invaginations we have observed are associated with actin, we conducted adjacent-face double-localization experiments using anti-actin and anti-Ste2p antibodies (see MATERIALS AND METHODS).

These double-localization experiments were done on adjacent-face pairs of cell sections obtained from samples not exposed to  $\alpha$ -factor ( $t = 0$  min) and briefly exposed ( $t = 5$  min) to  $\alpha$ -factor. Digital images of anti-Ste2p localizations to the furrow-like invaginations were acquired, and then digital images of the matching cell sections that had been incubated with anti-actin antibodies were acquired. These digital pairs were merged and examined for colocalization of Ste2p and actin at the furrow-like invaginations. As can be seen in Figure 6, Ste2p and actin were both observed on the furrow-like invaginations both before and after exposure to  $\alpha$ -factor. This colocalization was sometimes observed on small vesicles that were associated with, and perhaps pinching off, the furrow-like

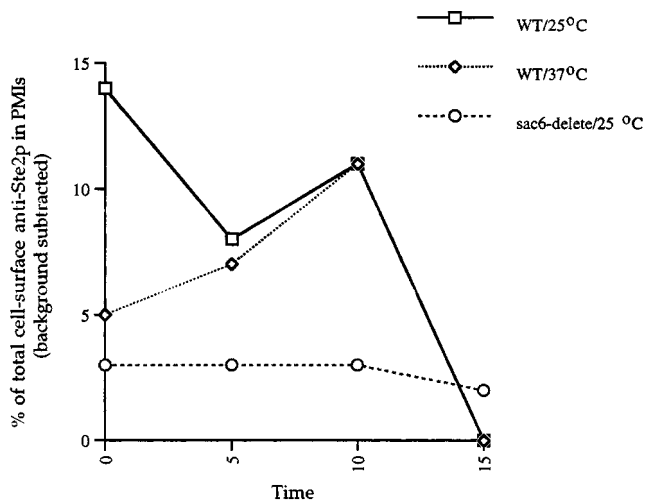


**Figure 5.** Ste2p is nonrandomly distributed between invaginated and noninvaginated areas of the cell surface. Percentage of cell surface-associated Ste2p that is in furrow-like plasma membrane invaginations (PMIs) in wild-type cells exposed to  $\alpha$ -factor at 25 or 37°C and *sac6* $\Delta$  cells at 25°C is plotted. A total of 50 individual cell sections at each time point were counted for each sample. Background localization to invaginations was  $33 \pm 2.4\%$  (averaged over all points) of the total cell surface background localization; this was subtracted from all data points shown.

invaginations (for examples, see Figure 6, B and C). However, not all Ste2-positive furrow-like invaginations showed actin localization. The failure to observe colocalization in every case may reflect limitations inherent in our technique (see MATERIALS AND METHODS).

Together these results show that in wild-type cells Ste2p is nonrandomly distributed over the yeast plasma membrane, with Ste2p being concentrated in furrow-like invaginations. Furthermore, this differential distribution of Ste2p at the cell surface appears to be maintained during receptor-mediated endocytosis. Consistent with a role in endocytosis, we have also shown that actin colocalizes with many of the furrow-like invaginations that contain Ste2p.

#### *Internalized Ste2p Is Located in Prevacuole Endosomes*

Previous studies demonstrated that the endocytic pathway in yeast converges with a branch of the exocytic pathway in a prevacuolar compartment (reviewed in Bryant and Stevens, 1998). These studies have shown, by various methods, that both the vacuolar protease CPY and the vacuolar ATPase Vph1p are sorted from a late Golgi compartment and transported, via a prevacuolar compartment, to the yeast vacuole. This prevacuole compartment contains the Golgi-modified, proenzyme forms of these vacuolar proteins. In cell fractionation studies this compart-

ment contains both Ste2p and the Golgi-modified, proenzyme form of CPY. Thus, this prevacuole compartment has been implicated as a component of the endocytic pathway (Piper *et al.*, 1995).

In immuno-EM experiments using wild-type cells not exposed to  $\alpha$ -factor we observed that affinity-purified antibodies generated against CPY and the 90-kDa subunit of Vph1p labeled, as expected, the yeast vacuole as well as membrane-bound compartments located near the vacuole (Figure 7). These compartments were indistinguishable in appearance from the Ste2p-containing perivacuole compartments we had observed predominately in cells exposed to  $\alpha$ -factor for 10 and 15 min (see Figure 3).

In yeast, the rab5 homologue Ypt51p (Vps21p) has been shown to be required for both endocytic transport (Singer-Kruger *et al.*, 1994; Singer-Kruger *et al.*, 1995) and for proper sorting of vacuolar hydrolases from the exocytic pathway (Horazdovsky *et al.*, 1994). In immunofluorescence microscopy, Ypt51p localizes to multiple punctate compartments, and subcellular fractionation studies indicate that Ypt51p is associated with endocytic intermediates but not with the late Golgi compartment (Singer-Kruger *et al.*, 1995). Therefore, to determine whether these perivacuole compartments were endosomal and not Golgi intermediates, we conducted additional immuno-EM experiments on wild-type cells using affinity-purified antibodies directed against Ypt51p (Singer-Kruger *et al.*, 1995).

We found that affinity-purified anti-Ypt51 antibodies did indeed localize to perivacuole compartments that were morphologically indistinguishable from those to which we had previously located Ste2p, CPY, and Vph1p (Figure 7). However, the level of anti-Ypt51p antibody localization to these compartments was relatively low, presumably because of the low abundance of Ypt51p therein (Singer-Kruger *et al.*, 1994). Nevertheless, this result, together with the localization of CPY, Vph1p, and Ste2p, suggests that these perivacuolar compartments are most likely prevacuolar endosomes.

To further define these perivacuolar compartments as yeast prevacuolar endosomes, we conducted double-labeling immuno-EM experiments using our adjacent-face double-localization technique. Because colocalization of Ste2p and CPY has been used to define the prevacuole endosomal compartment in cell fractionation studies, we used antibodies directed against these same markers. Double-label experiments were done on cell section pairs obtained from wild-type samples exposed to  $\alpha$ -factor for 10 and 15 min at 25°C.

To determine the fraction of CPY-positive perivacuolar compartments that contain Ste2p, we acquired images of cell sections that had CPY immunogold localization to these compartments. Because these compartments have a characteristic electron density (for examples, see Figures 3 and 7) they were easy to

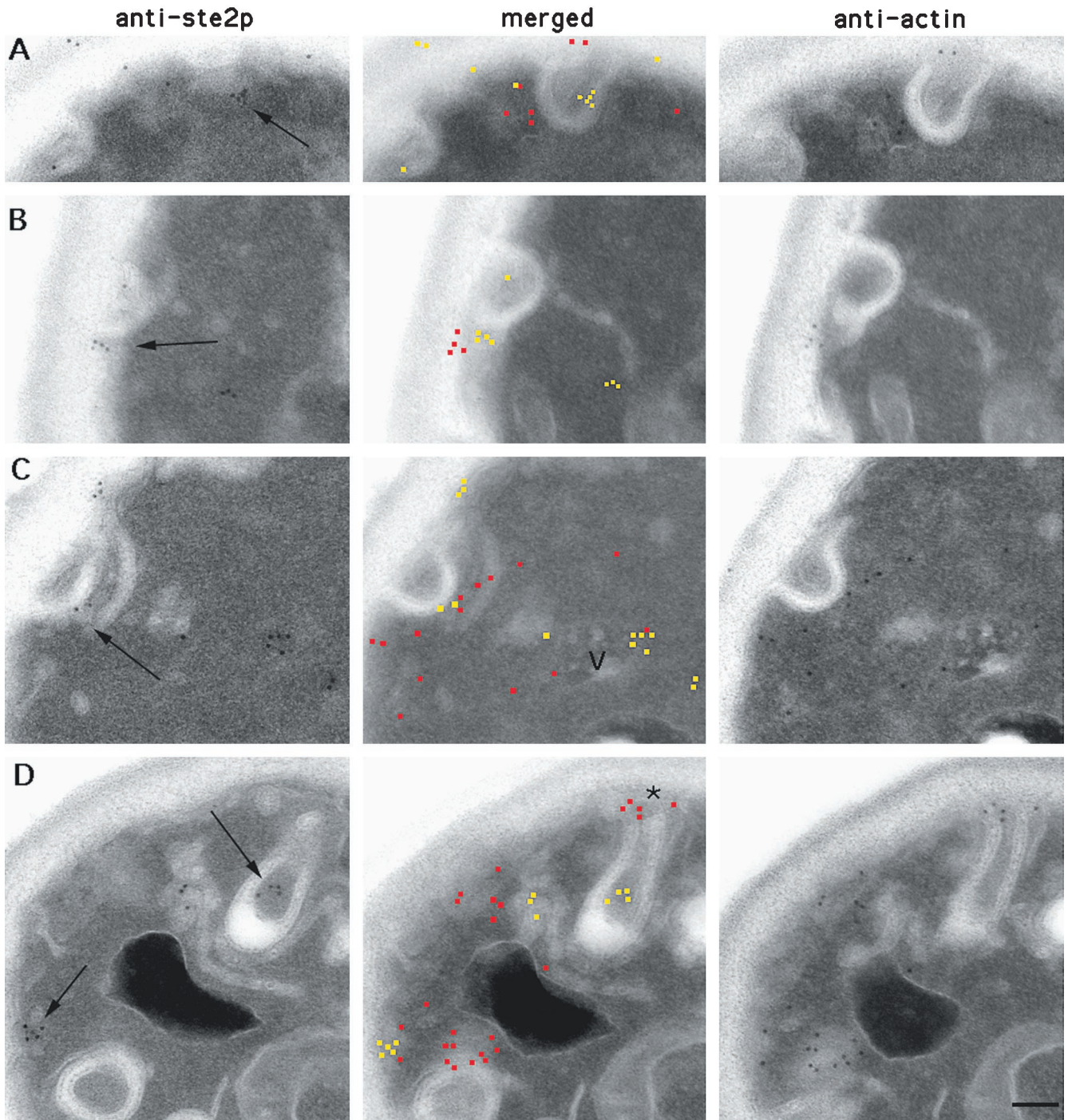


**Figure 6.** Ste2p (yellow in merged image) is localized to vesicles that are proximal and perhaps continuous with furrow-like invaginations of the plasma membrane (arrows) and colocalizes with actin (red in merged image). Adjacent-face double localization of Ste2p and actin in wild-type cells before (A and B) and after ( $t = 5$  min; C and D) exposure to  $\alpha$ -factor is shown. Note that the anti-Ste2p section in A does not appear to be associated with a plasma membrane invagination until the adjacent section is examined. Note also in D that the “tip” of the furrow-like invagination (asterisk) has anti-actin antibodies localized around it. Bar, 0.1  $\mu$ m.

identify; only those marker-positive compartments of  $\sim 100$  nm or larger were counted. The matching cell

sections that had been incubated with anti-Ste2p antibodies were then acquired, and the anti-CPY and anti-

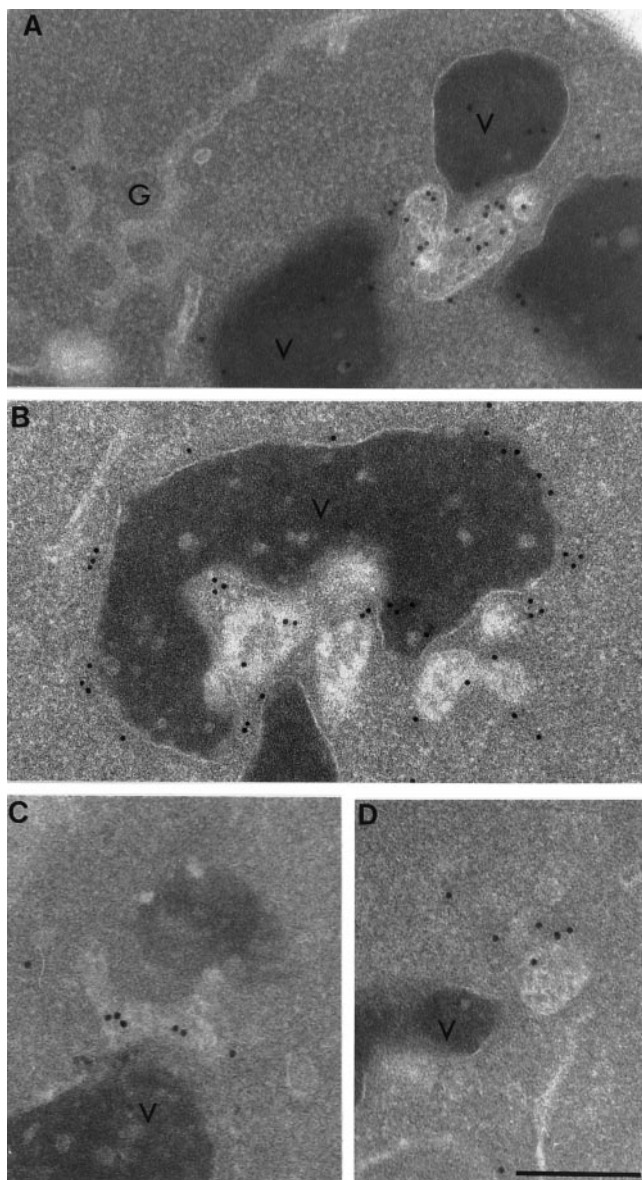


**Figure 7.** Antibodies directed against the vacuolar protease CPY (A) and the 90-kDa subunit of the vacuolar H<sup>+</sup> ATPase Vph1p (B) localize to the vacuole and vacuole-associated compartments in wild-type cells. Note that the anti-CPY antibodies localize within the vacuole and the vacuole-associated compartment and that anti-Vph1p antibodies localize to the membrane of the vacuole and the perivacuole compartment. These perivacuole compartments, but not the vacuole, localize antibodies directed against Ypt51p (C and D). Note that the vacuole-associated compartments appear as tubular-vesicular structures having internal membranes. V, vacuole; g, Golgi. Bar, 0.5  $\mu$ m.

Ste2p immunogold pairs were then compared. Figure 8 shows two typical anti-Ste2p, anti-CPY adjacent-face localization results. From the cells incubated for 10 min in  $\alpha$ -factor we acquired 14 images of anti-CPY-positive perivacuolar compartments of which 11, or

79%, showed a corresponding localization of anti-Ste2p immunogold. At  $t = 15$  min we observed 38 anti-CPY-positive perivacuolar compartments of which 33, or 87%, showed a corresponding localization of anti-Ste2p immunogold.

The percentage of Ste2p-containing endosomes that also contained CPY was also determined by acquiring images of anti-Ste2p-positive perivacuolar compartments and then acquiring the matching cell section incubated with anti-CPY antibodies. From the sample exposed to  $\alpha$ -factor for  $t = 10$  min we acquired 11 images of anti-Ste2p-positive perivacuolar compartments of which 8, or 73%, showed a corresponding localization of anti-CPY immunogold. At  $t = 5$  min we observed 50 anti-Ste2p-positive perivacuolar compartments of which 38, or 76%, showed a corresponding localization of anti-CPY immunogold.

To determine the false-negative rate for our adjacent-face double-localization technique, (i.e., what percentage of our double-label cell section pairs fail to show colocalization when colocalization is expected), we conducted the following control. Adjacent-face cell section pairs were obtained from our wild-type ( $t = 10$  min) sample, and both adjacent faces were exposed to antibodies directed against Ste2p. We acquired images of perivacuolar compartments to which anti-Ste2p immunogold had localized and then acquired images of the matching cell sections. Of 30 Ste2p-positive compartments thus obtained, 6 did not show a corresponding Ste2p signal on the perivacuolar compartment observed in the adjacent cell section. Thus, the false-negative rate for anti-Ste2p antibodies in our adjacent-face double-label technique is  $\sim 20\%$ .

Together these results indicate that at 10 and 15 min after exposure to  $\alpha$ -factor essentially all of the observed perivacuolar compartments contain both endocytosed Ste2p and CPY. Interestingly, examination of the cell section pairs also revealed that these compartments contain vesicle-like membrane profiles to which Ste2p was localized (Figure 8C). Therefore, we conclude that these compartments are indeed the prevacuole endosomal compartments previously identified in cell fractionation studies. This compartment appears morphologically similar to its mammalian counterpart.

#### *The Prevacuole Compartment Is a Late Endosome*

Using an improved, multistep purification procedure, Singer-Kruger *et al.* (1993) kinetically resolved and purified two distinct endosomal fractions from wild-type yeast cells. Internalized  $\alpha$ -factor fractionated with these two biochemically separable, membrane-bound compartments in a temperature- and time-dependent manner. Thus, at reduced temperature, internalized  $\alpha$ -factor can be observed first in a heavy-density fraction and then in a second, lighter-density fraction.

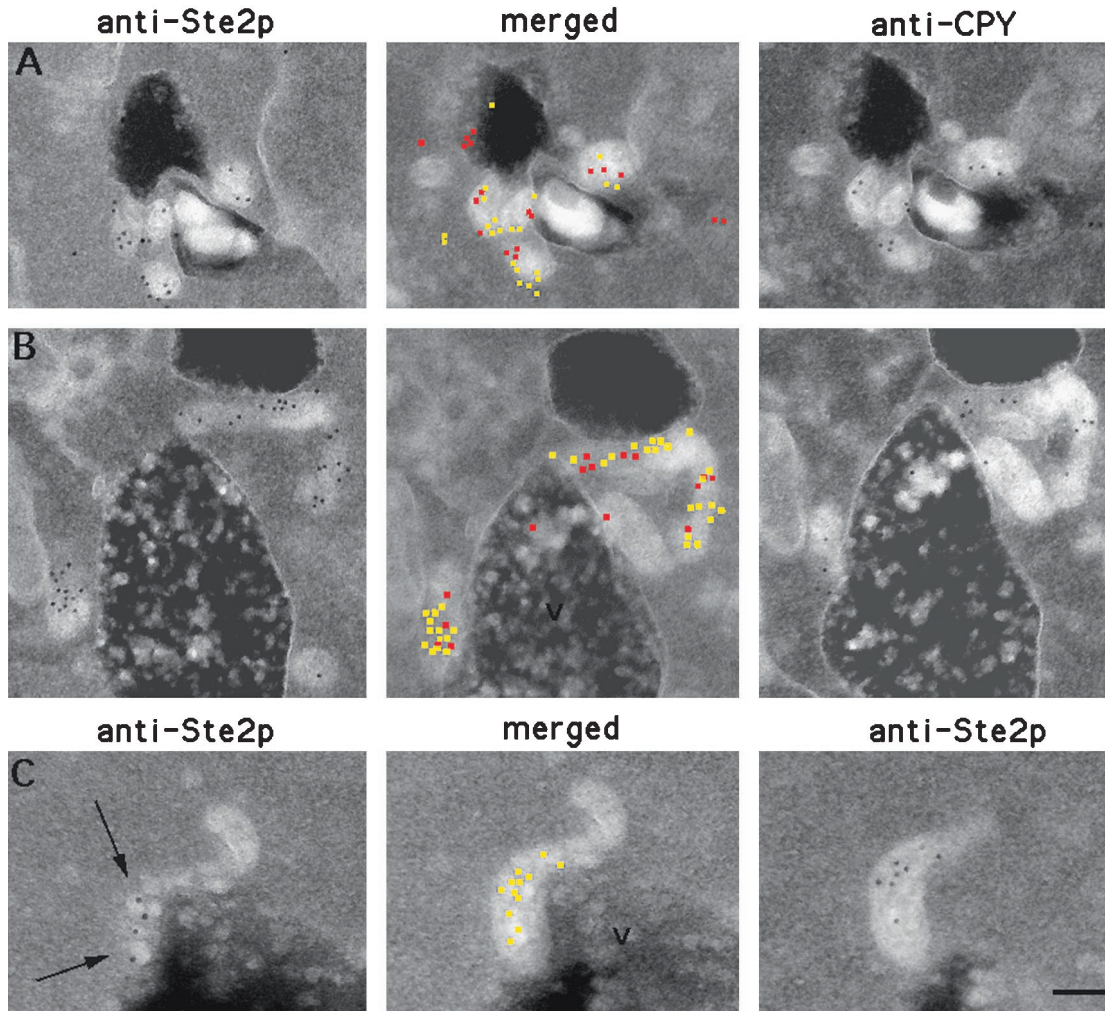


**Figure 8.** CPY and internalized Ste2p colocalize in prevacuole compartments. (A and B) Adjacent-face double localization of anti-Ste2p (yellow in merged images) and anti-CPY (red in merged images) antibodies after 15 min of continuous exposure to  $\alpha$ -factor at 25°C. Note that the prevacuole compartments appear to be interconnected. (C) Example of adjacent-face double labeling with Ste2p antibodies only. Note that the first section of C shows a grazing cut through a prevacuole compartment that contains vesicles to which Ste2p is localized (arrows). This prevacuole compartment appears to be fusing with the vacuole. V, vacuole. Bar, 0.1  $\mu$ m.

These two kinetically distinct fractions are inferred to contain early and late endosomal compartments, respectively.

We reasoned that, if the perivacuolar compartments we have identified as prevacuolar (CPY<sup>+</sup>, Ste2p<sup>+</sup>) endosomes are the *in vivo* counterpart of the *in vitro*-defined late endosome, then it should be possible to observe, in wild-type cells, a ligand- and time-dependent increase in the number of these Ste2p-positive compartments. More importantly, because endosomal transport of internalized  $\alpha$ -factor is rapid, localization to these endosomes should peak, in wild-type cells, ~10–15 min after exposure to  $\alpha$ -factor (Hicke *et al.*, 1997). It is also expected that the number of CPY-containing prevacuole endosomes should be at a steady-state level, and the number of Ste2p-containing

compartments should converge on this number after exposure to  $\alpha$ -factor. Therefore, to confirm that these prevacuole endosomes are indeed yeast late endosomes, we conducted the following immuno-EM experiments.

We immunolocalized Ste2p to sections cut from wild-type samples that had been exposed to  $\alpha$ -factor for 0, 5, 10, or 15 min at 25°C. At each time point we observed a total of 300 cell sections and recorded the number of cell sections that contained anti-Ste2p-positive prevacuole endosomes as well as the total number of Ste2p-positive prevacuole endosomes observed within those cell sections. This experiment was then repeated with antibodies directed against CPY.

As can be seen in Figure 9A, the percentage of cell sections that contained CPY-positive endosome(s) re-

mained relatively constant after exposure to  $\alpha$ -factor at 25°C. In contrast, the percentage of cell sections that contained Ste2p-positive endosome(s) steadily increased for the first 10 min after exposure to  $\alpha$ -factor, after which it plateaued. The same is true for the total number of marker-positive endosomes we observed at each time point; this is plotted in Figure 9B as the average number of endosomes observed per cell section. In the Ste2p localization experiment we observed a steady increase in the total number Ste2p-positive endosomes after exposure to  $\alpha$ -factor, leveling out at 10 min. Again, in the CPY localization experiment we observed a relatively constant number of CPY-positive endosomes. Importantly, the percentage of cell sections with CPY- and Ste2p-positive endosomes as well as the average number of CPY- and Ste2p-positive endosomes converged at  $t = 10$  min, as predicted for late endosome compartments. Thus, we conclude that, in yeast, the CPY- and Ste2p-containing prevacuolar compartments are late endosomes.

#### Wild-Type Cells Accumulate Late Endosomes at 37°C

We noted above an apparent temperature-dependent increase in the number of endosomal compartments and the degree of their labeling in wild-type cells incubated in the presence of  $\alpha$ -factor at 37°C (see Figure 3). This suggests the possibility that this compartment accumulates as a result of heat shock, consistent with a role in dealing with misfolded proteins. To quantitate this observation we repeated the experiments on cell sections taken from wild-type samples just before ( $t = 0$  min) and after ( $t = 5, 10,$  and  $15$  min) incubation with  $\alpha$ -factor at 37°C. Before addition of  $\alpha$ -factor, all four samples were preshifted to 37°C for 15 min.

At 37°C the percentage of cell sections that contained CPY-positive endosome(s) remained relatively constant after exposure to  $\alpha$ -factor at 37°C, and this level was similar to that observed at 25°C (Figure 9). In contrast to the 25°C analysis, however, the percentage of cell sections that contained Ste2p-positive endosome(s) was already at the CPY-positive endosome level at  $t = 0$  min and remained there after exposure to  $\alpha$ -factor (Figure 9). When we quantitated the total number of marker-positive endosomes at 37°C, we observed a large increase in the total number; at 37°C, just before  $\alpha$ -factor exposure, the number of CPY-positive endosomes was  $\sim 1.5$  times the 25°C level. Similarly, the total number of Ste2p-positive endosomes was  $\sim 2.6$  times the 25°C level. Importantly, as in the 25°C samples, the number of CPY-positive endosomes remained constant, and the number of Ste2p-positive endosomes converged with the CPY level within 10 min of exposure to  $\alpha$ -factor at 37°C.

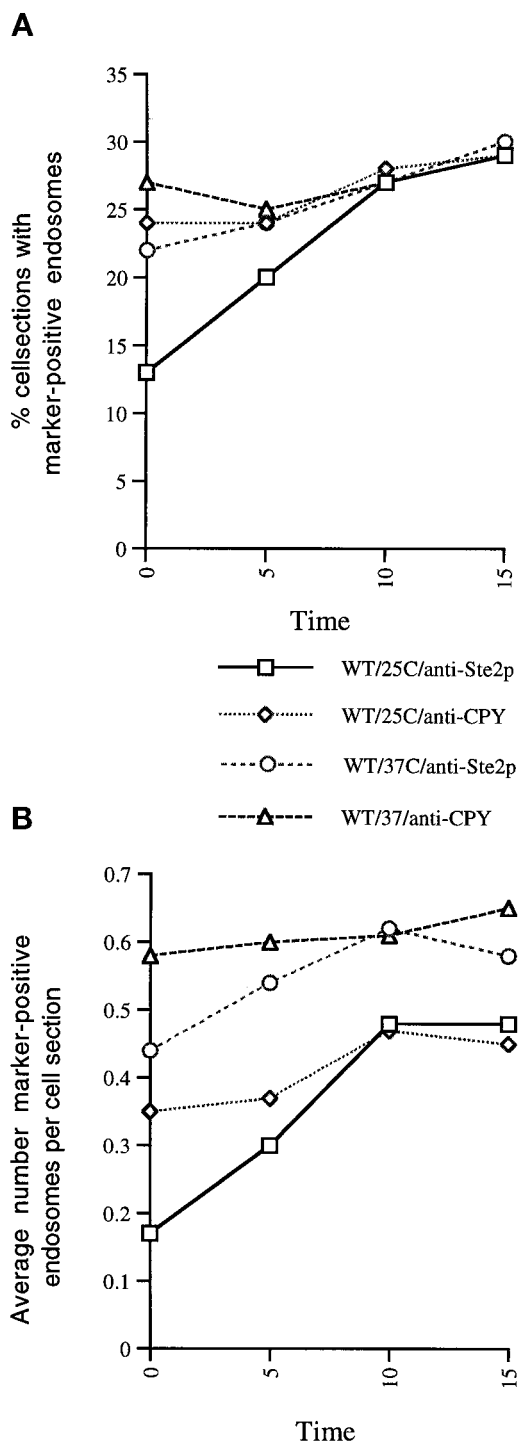


**Figure 9.** Prevacuole compartments are late endosomes. Quantitation of Ste2p and CPY in prevacuole compartments after exposure to  $\alpha$ -factor at 25 or 37°C. For each time point 300 cell sections were observed, and the number of CPY- or Ste2p-containing endosomes was counted. (A) Percentage of cell sections that were observed with CPY or with Ste2p antibody localization. (B) Average number of marker-positive (Ste2p or CPY) endosomes that were observed within those cell sections.

To confirm that our 37°C samples had not been subject to a preshift condition that could have caused the observed perturbation of the endocytic pathway, we quantitated anti-Ste2p localization to the 25°C grown sample ( $t = 0$  min) that had been taken just before the 37°C preshift. At  $t = 0$  min we observed levels of anti-Ste2p localization to prevacuole endosomal compartments that were similar to those we observed in other samples of wild-type cells grown at 25°C before exposure to  $\alpha$ -factor. These results confirm our initial observation of a temperature-dependent accumulation and aggregation of these late endosomal compartments.

## DISCUSSION

We have shown that the receptor Ste2p is located on the yeast cell surface. In wild-type cells exposed to  $\alpha$ -factor, but not in the endocytosis defective mutant *sac6* $\Delta$ , we observed a rapid and quantitative loss of Ste2p from the cell surface. We also observed that, before and after exposure to  $\alpha$ -factor, Ste2p was nonrandomly distributed over the cell surface of wild-type cells and appeared to be concentrated in the furrow-like invaginations. This differential localization of Ste2p was not observed in *sac6* $\Delta$  cells.

Our observations extend to the ultrastructure level observations of nonrandom distribution of Ste2p over the surface. Hicke *et al.* (1997), using immunofluorescent confocal microscopy, showed that Ste2p is distributed in a spotty pattern over the yeast cell surface. After exposure to  $\alpha$ -factor ( $t = 4$  min), the cell surface Ste2p signal is diminished but still retains a spotty distribution at the periphery of the cell (Hicke *et al.*, 1997). In cells exposed briefly to  $\alpha$ -factor ( $t = 5$  min) we observed a loss of Ste2p from the cell surface but continued to observe Ste2p in furrow-like invaginations. Some of these invaginations were also associated with small, presumably endocytic, vesicles and tubular-vesicular endosomal structures that contained Ste2p. Thus, the spotty immunofluorescent localization of Ste2p can be explained by the localization of Ste2p in furrow-like plasma membrane invaginations as well as after exposure to  $\alpha$ -factor in early endocytic structures that are located proximal to these structures.

Interestingly, Wendland *et al.* (1996) demonstrated quantitatively, using a ferritin-based assay for fluid-phase endocytosis, that spheroplasted (i.e., cells with the cell wall removed) *she4* and *pan1* mutants accumulate ferritin in aberrantly long invaginations of the plasma membrane. Cells defective in *SHE4* or *PAN1* function have defects in both actin cytoskeleton organization and endocytosis. More recently Singer-Kruger *et al.* (1998) demonstrated that deletion of two of the yeast synaptojanin homologues, *SJL1* and *SJL2*, resulted in defects in receptor-mediated endocytosis

and actin cytoskeleton organization. EM examination of the *sjl1*, *sjl2* double-mutant cells revealed abnormally deep invaginations of the plasma membrane, reminiscent of those observed in *she4* and *pan1* mutants. Interestingly, deletion of *SJL1*, but not *SJL2*, has been shown to be synthetically lethal with an allele of *PAN1* (Wendland and Emr, 1998). Pan1p is required for endocytosis and may function, via its two eps15 homology domains, as a multivalent adaptor protein.

Recently, Prescianotto-Baschong and Riezman (1998) followed the constitutive uptake of positively charged gold particles (nanogold) to define endocytic compartments in yeast spheroplasts incubated at 15°C. They observed nanogold particles over the cell surface, including shallow plasma membrane invaginations, and intracellular compartments. Whether the invaginations and intracellular compartments identified by Prescianotto-Baschong and Riezman (1998) are the same as the ones to which we have located Ste2p is unclear. This is because the internalization conditions, state of the cells, and EM methods used to follow the constitutive uptake of nanogold are significantly different from the immuno-EM methods we have used to follow the ligand-dependent uptake of Ste2p. Thus, direct comparison of results obtained with these two different methods is not feasible.

### Role of the Actin Cytoskeleton

Many components of the actin cytoskeleton, as well as many of the proteins that are expected to interact with the actin cytoskeleton, appear to be required for the internalization step(s) of endocytosis. These include actin itself, Sla2p (End4p), fimbrin (Sac6p), cofilin, Arp2, Rvs161p (End6p), Rvs167, verprolin (End5p), Rvs167p, End3p, and Pan1 (Dim2p), both of which contain eps15 homology domains, as well as calmodulin and type I Myo5p (Kubler and Riezman, 1993; Raths *et al.*, 1993; Benedetti *et al.*, 1994; Munn *et al.*, 1995; Wendland *et al.*, 1996; Moreau *et al.*, 1997; Tang *et al.*, 1997; Wesp *et al.*, 1997; Geli and Riezman, 1996; Geli *et al.*, 1998; Wendland and Emr, 1998). Interestingly, several proteins that have been localized specifically to the actin cortical patch and not to actin cables have been shown to be required for endocytosis.

At the ultrastructural level the cortical actin patch appears as a finger-like invagination of the plasma membrane around which actin and actin-binding proteins are organized (Mulholland *et al.*, 1994). Additionally, the cortical actin patch, although generally restricted to areas of active cell growth, has been shown to be highly mobile and can move at speeds of 0.1–0.5  $\mu\text{m/s}$  (Doyle and Botstein, 1996; Waddle *et al.*, 1996). Thus, the cortical actin patch, known to contain proteins genetically implicated in endocytosis, became an obvious candidate for mediating endocytosis.

Using double-localization techniques we tested this hypothesis by looking for colocalization of Ste2p with the cortical actin patch. We used antibodies directed against the cortical patch marker cofilin as well as against actin itself together with anti-Ste2p antibodies. We observed ~240 cortical patches and surprisingly did not observe any significant colocalization of Ste2p with the cortical actin patch before or after exposure to  $\alpha$ -factor. Thus, we are led to the conclusion that Ste2p is not internalized through the finger-like invagination of the cortical patch.

There remains a formal possibility, however, that we might fail to observe colocalization of Ste2p and the cortical actin patch because of the speed at which the actin patch moves relative to the kinetics of Ste2p internalization. Consistent with this possibility, we did occasionally observe cortical actin patches that appeared to be associated with Ste2p-containing plasma membrane invaginations (for examples, see Figure 4). On the other hand, it should be recalled that cortical actin patches are concentrated at areas of active cell growth, whereas Ste2p-containing invaginations appear to be more evenly distributed (Hicke *et al.*, 1997; this study). Thus the appealing idea that the actin cytoskeleton functions in endocytosis via the actin cortical patch is rendered unlikely. Instead, we favor a model in which the actin cytoskeleton's effect on endocytosis is exerted, possibly more indirectly, through other cortical structures such as the long furrows described above.

Consistent with the expectation that the actin cytoskeleton is nevertheless functionally associated with the sites of Ste2p internalization, we did observe limited colocalization of actin and Ste2p on the furrow-like invaginations of the plasma membrane, and these invaginations are distinct from the finger-like invaginations of the cortical actin patch (Mulholland *et al.*, 1994). On occasion this colocalization was too small, Ste2p-containing, and thus presumably endocytic vesicles that were directly adjacent to a furrow-like invagination (see Figure 6).

Collectively, these data suggest that the furrow-like invaginations are the site of Ste2p internalization. These invaginations label, albeit weakly, with anti-actin antibodies, and as we have demonstrated here, are distinct from the finger-like invaginations previously shown to be components of the cortical actin patch (Mulholland *et al.*, 1994). However, because most, if not all, of the yeast actin cytoskeleton is located at or near the cell surface, we could not determine in wild-type cells whether the association of actin (and the occasional cortical actin patch) with the furrow-like invaginations is functionally significant. It also remains unclear whether the aberrant invaginations observed in some endocytosis mutants result directly from a failure to endocytose. Further characterization of the internalization step(s) of receptor-

mediated endocytosis, particularly with respect to the role of the actin cytoskeleton and invaginations of the plasma membrane, will require the use of mutants that are defective in the internalization of Ste2p.

#### *Characterization of the Yeast Prevacuole/Late Endosome*

We observed intense Ste2p localization in prevacuole compartments that have an internal morphology suggestive of membranes and appear to be most similar to the late endosomes of animal cells. Using immuno-EM we showed that these prevacuole compartments contain the vacuolar proteins CPY and Vph1p and, significantly, the rab/Ypt protein Ypt51p (Vps21p), although at steady state, association with the compartment may no longer reflect Ypt51p function. Furthermore, using our adjacent-face double-labeling technique we showed, in cells exposed to  $\alpha$ -factor for 10 and 15 min, that these morphologically distinct prevacuole compartments contain both CPY and internalized Ste2p. Thus, the multivesicular, prevacuolar compartments we have visualized represent the convergence of the degradative and biosynthetic pathways and are, therefore, yeast prevacuole compartments (Raymond *et al.*, 1992; Piper *et al.*, 1995; Rieder *et al.*, 1996).

Internalization and transport of Ste2p to the yeast vacuole is rapid and it is expected that after 10 min of exposure to  $\alpha$ -factor, internalized Ste2p will be located in an *in vivo* endosomal compartment that corresponds to the kinetically defined *in vitro* late endosome (Singer-Kruger *et al.*, 1993; Hicke *et al.*, 1997). In our experiments we showed that the prevacuole (CPY<sup>+</sup>) compartments accumulate Ste2p in a time- and ligand-dependent manner. After exposure to  $\alpha$ -factor we could observe an increase in the number of prevacuole compartments and an increase in the degree with which they labeled with Ste2p antibodies. In contrast, the number of CPY-containing prevacuole compartments remained relatively constant. This constant level of CPY-containing prevacuole compartments is expected to represent the wild-type steady-state level of these compartments. Importantly, we observed that the number of Ste2p-containing prevacuole compartments equaled the steady-state level of the CPY-containing compartments after 10 min of exposure to  $\alpha$ -factor. This result is consistent with the observed kinetics of  $\alpha$ -factor arrival in the biochemically defined late endosomal intermediate. Thus, we conclude that these prevacuole (Ste2p<sup>+</sup>, CPY<sup>+</sup>) compartments are the *in vivo* counterparts of the *in vitro*-defined late endosome.

In wild-type cells incubated with  $\alpha$ -factor at 37°C, we observed an extraordinary time-dependent increase in the number of these late endosomes and in the degree of their labeling. Furthermore, we ob-

served, with about the same frequency, cell sections that contained marker-positive endosomes at 25 and 37°C. But surprisingly, we observed, at 37°C compared with 25°C, an increased number of these late endosomes in those cell sections. This is consistent with the idea that late endosomes are not randomly distributed throughout the cytoplasm but rather tend to form aggregates that are located next to the vacuole. Furthermore, this result demonstrates that late endosomes can accumulate and, thus, suggests that these compartments are transport intermediates. The observation that some late endosomes appear to be fusing directly with the yeast vacuole further supports this idea.

Immunofluorescent microscopy observation of cells treated with cycloheximide has revealed an apparently similar accumulation of perivacuole (presumably late endosomal) compartments (Hicke *et al.*, 1997). In those cells,  $\alpha$ -factor degradation was also shown to be greatly delayed. Thus, it appears that continuous synthesis of new proteins is required for endosomal transport. This result suggests the following explanation for the temperature-induced perturbation of the endosomal system. High, nonphysiological temperatures may cause a transient overproduction of misfolded proteins. These misfolded proteins must be transported to the yeast vacuole for degradation. This overproduction saturates the endosomal pathway presumably by titrating out required transport proteins. Thus in both cases, heat shock and inhibition of protein synthesis, there may exist a shortage of critical endosomal proteins. However, whatever the reason, the temperature-induced perturbation of the endosomal pathway underscores the fact that temperature shifts are physiologically stressful and can disrupt subcellular pathways even in wild-type cells.

#### *Adjacent Face Double-Label Immuno-EM*

It should be clear that our results would not have been quite so clear had we been unable to do double-label experiments or were limited to techniques using alternative species to raise antibodies or weak blocking systems. We suggest that our adjacent-face double-labeling technique may have wide application, not least because the labeling is limited to the materials that are immediately touching before they are sectioned. Using this technique we have been able to make inferences (e.g., the situations produced by cuts that graze a structure) that would have been difficult or impossible with other techniques.

#### *Conclusion*

The process of receptor-mediated endocytosis in mammalian and yeast cells is in large part con-

served between yeast and animal cells. Indeed, many of the same proteins that mediate internalization and endosomal transport in mammalian cells have been found to function analogously in yeast cells.

The direct observation of ligand-induced, receptor-mediated endocytosis and the ultrastructural identification of authentic endosomal compartments in yeast provide additional evidence for this conservation of mechanism. Furthermore, they provide a genetically tractable system in which to directly correlate endocytic structure with the molecular determinants of endocytic function. Thus, the internalization assay and techniques presented here, together with the use of appropriate endocytosis mutants, will now allow further dissection of receptor internalization and endosomal transport in yeast.

#### ACKNOWLEDGMENTS

We thank George and Camilla Smith for generous gifts allowing us to establish and maintain an EM facility. We thank Andreas Wesp for comments. Thanks to Elizabeth Jones for the gift of affinity-purified antibodies directed against CPY and Vph1p. We also acknowledge the capable engineers at Gatan for custom installing a Bioscann CCD camera on our vintage Philips 300 electron microscope. Finally, we thank two anonymous reviewers for their insistence that double-label experiments be done. This research was supported by National Institutes of Health grant GM-46406.

#### REFERENCES

- Adams, A.E., Botstein, D., and Drubin, D. (1991). Requirement of yeast fimbrin for actin organization and morphogenesis *in vivo*. *Nature* 354, 404–408.
- Anderson, R., Vasile, E., Mello, R., Brown, M., and Goldstein, J. (1978). Immunocytochemical visualization of coated pits and vesicles in human fibroblasts: relation to low density lipoprotein receptor distribution. *Cell* 15, 919–933.
- Benedetti, H., Raths, S., Crausaz, F., and Riezman, H. (1994). The *END3* gene encodes a protein that is required for the internalization step of endocytosis and for actin cytoskeleton organization in yeast. *Mol. Biol. Cell* 5, 1023–1037.
- Botstein, D., Amberg, D., Huffaker, T., Mulholland, J., Adams, A., Drubin, D., and Stearns, T. (1997). The yeast cytoskeleton. In: *The Molecular and Cellular Biology of the Yeast Saccharomyces*, ed. J.R. Broach, J.R. Pringle, and E.W. Jones, Cold Spring Harbor, NY: Cold Spring Harbor Laboratory, 1–90.
- Bryant, N., and Stevens, T. (1998). Vacuole biogenesis in *Saccharomyces cerevisiae*: protein transport pathways to the yeast vacuole. *Microbiol. Mol. Biol. Rev.* 62, 230–247.
- Chvatchko, Y., Howald, I., and Riezman, H. (1986). Two yeast mutants defective in endocytosis are defective in pheromone response. *Cell* 46, 355–364.
- Davis, N.G., Horecka, J.L., and Sprague, G.F., Jr. (1993). Cis- and trans-acting functions required for endocytosis of the yeast pheromone receptors. *J. Cell Biol.* 122, 53–65.

- Doyle, T., and Botstein, D. (1996). Movement of yeast cortical actin cytoskeleton visualized in vivo. *Proc. Natl. Acad. Sci. USA* 93, 3886–3891.
- Drubin, D., Miller, K., and Botstein, D. (1988). Yeast actin-binding proteins: evidence for a role in morphogenesis. *J. Cell Biol.* 107, 2551–2561.
- Dulic, V., and Riezman, H. (1989). Characterization of the *END1* gene required for vacuole biogenesis and gluconeogenic growth of budding yeast. *EMBO J.* 8, 1349–1359.
- Geli, M., and Riezman, H. (1996). Role of type I myosins in receptor-mediated endocytosis in yeast. *Science* 272, 533–535.
- Geli, M., and Riezman, H. (1998). Endocytic internalization in yeast and animal cells: similar and different. *J. Cell Sci.* 111, 1032–1037.
- Geli, M., Wesp, A., and Riezman, H. (1998). Distinct functions of calmodulin are required for the uptake step of receptor-mediated endocytosis in yeast: the type I myosin Myo5p is one of the calmodulin targets. *EMBO J.* 17, 635–647.
- Givan, S., and Sprague, G. (1997). The ankyrin repeat-containing protein Akr1p is required for the endocytosis of yeast pheromone receptors. *Mol. Biol. Cell* 8, 1317–1327.
- Goldstein, J., Anderson, R., and Brown, M. (1979). Coated pits, coated vesicles, and receptor-mediated endocytosis. *Nature* 279, 679–685.
- Hicke, L., Zanolari, B., Pypaert, M., Rohrer, J., and Riezman, H. (1997). Transport through the yeast endocytic pathway occurs through morphologically distinct compartments and requires an active secretory pathway and Sec18p/N-ethylmaleimide-sensitive fusion protein. *Mol. Biol. Cell* 8, 13–31.
- Horazdovsky, B.F., Busch, G.R., and Emr, S.D. (1994). VPS21 encodes a rab5-like GTP binding protein that is required for the sorting of yeast vacuolar proteins. *EMBO J.* 13, 1297–1309.
- Jackson, C., Konopka, J., and Hartwell, L. (1991). *S. cerevisiae* alpha pheromone receptors activate a novel signal transduction pathway for mating partner discrimination. *Cell* 67, 389–402.
- Jenness, D., and Spatrick, P. (1986). Down-regulation of the alpha-factor pheromone receptor in *S. cerevisiae*. *Cell* 46, 345–353.
- Konopka, J., Jenness, D., and Hartwell, L. (1988). The C-terminus of the *S. cerevisiae* alpha-factor pheromone receptor mediates an adaptive response to pheromone. *Cell* 54, 609–620.
- Kubler, E., and Riezman, H. (1993). Actin and fimbrin are required for the internalization step of endocytosis in yeast. *EMBO J.* 12, 2855–2862.
- Kubler, E., Schimmoller, F., and Riezman, H. (1994). Calcium-independent calmodulin requirement for endocytosis in yeast. *EMBO J.* 13, 5539–5546.
- Lappalainen, P., and Drubin, D. (1997). Cofilin promotes rapid actin filament turnover in vivo. *Nature* 388, 78–82.
- Manolson, M., Proteau, D., Preston, R., Stenbit, A., Roberts, T.B., Hoyt, M.A., Preuss, D., Mulholland, J., Botstein, D., and Jones, E. (1992). The *VPH1* gene encodes a 95-kDa integral membrane polypeptide required for in vivo assembly and activity of the yeast vacuolar H<sup>+</sup>-ATPase. *J. Biol. Chem.* 267, 14294–14303.
- Moon, A., Janmey, P., Louie, K., and Drubin, D. (1993). Cofilin is an essential component of the yeast cortical cytoskeleton. *J. Cell Biol.* 120, 421–435.
- Moreau, V., Galan, J.M., Devillers, G., Haguenaer-Tsapis, R., and Winsor, B. (1997). The yeast actin-related protein Arp2p is required for the internalization step of endocytosis. *Mol. Biol. Cell* 8, 1361–1375.
- Mukherjee, S., Ghosh, R., and Maxfield, F. (1997). Endocytosis. *Physiol. Rev* 77, 759–803.
- Mulholland, J., Preuss, D., Moon, A., Wong, A., Drubin, D., and Botstein, D. (1994). Ultrastructure of the yeast actin cytoskeleton and its association with the plasma membrane. *J. Cell Biol.* 125, 381–391.
- Munn, A., and Riezman, H. (1994). Endocytosis is required for the growth of vacuolar H<sup>+</sup>-ATPase-defective yeast: identification of six new *END* genes. *J. Cell Biol.* 127, 373–386.
- Munn, A., Stevenson, B., Geli, M., and Riezman, H. (1995). *end5*, *end6*, and *end7*: mutations that cause actin delocalization and block the internalization step of endocytosis in *Saccharomyces cerevisiae*. *Mol. Biol. Cell* 6, 1721–1742.
- Nakagawa, Y., Tanaka, K., and Yanagishima, N. (1983). Occurrence of plasma membrane invaginations associated with sexual agglutination ability in the yeast *Saccharomyces cerevisiae*. *Mol. Gen. Genet.* 189, 211–214.
- Pearse, B.M. (1976). Clathrin: a unique protein associated with intracellular transfer of membrane by coated vesicles. *Proc. Natl. Acad. Sci. USA* 73, 1255–1259.
- Piper, R., Whitters, E., and Stevens, T. (1995). VPS27 controls vacuolar and endocytic traffic through a prevacuole compartment in *Saccharomyces cerevisiae*. *J. Cell Biol.* 131, 603–617.
- Prescianotto-Baschong, C., and Riezman, H. (1998). Morphology of the yeast endocytic pathway. *Mol. Biol. Cell* 9, 173–189.
- Raths, S., Rohrer, J., Crausaz, F., and Riezman, H. (1993). *end3* and *end4*: two mutants defective in receptor-mediated and fluid-phase endocytosis in *Saccharomyces cerevisiae*. *J. Cell Biol.* 120, 55–65.
- Raymond, C.K., Howald-Stevenson, I., Vater, C.A., and Stevens, T.H. (1992). Morphological classification of the yeast vacuolar protein sorting mutants: evidence for a prevacuolar compartment in class E vps mutants. *Mol. Biol. Cell* 3, 1389–1402.
- Rieder, S.E., Banta, L.M., Kohrer, K., McCaffery, J.M., and Emr, S.D. (1996). Multilamellar endosome-like compartment accumulates in the yeast vps28 vacuolar protein sorting mutant. *Mol. Biol. Cell* 7, 985–999.
- Rothberg, K., Heuser, J., Donzell, W., Ying, Y., Glenney, J., and Anderson, R. (1992). Caveolin, a protein component of caveolae membrane coats. *Cell* 68, 673–682.
- Schandel, K.A., and Jenness, D.D. (1994). Direct evidence for ligand-induced internalization of the yeast alpha-factor pheromone receptor. *Mol. Cell Biol.* 14, 7245–7255.
- Sherman, F., Fink, G., and Hicks, J. (1986). *Laboratory Course Manual for Methods in Yeast Genetics*, Cold Spring Harbor, NY: Cold Spring Harbor Laboratory.
- Singer, B., and Riezman, H. (1990). Detection of an intermediate compartment involved in transport of alpha-factor from the plasma membrane to the vacuole in yeast. *J. Cell Biol.* 110, 1911–1922.
- Singer-Kruger, B., Frank, R., Crausaz, F., and Riezman, H. (1993). Partial purification and characterization of early and late endosomes from yeast. Identification of four novel proteins. *J. Biol. Chem.* 268, 14376–14386.
- Singer-Kruger, B., Nemoto, Y., Daniwll, L., Ferro-Novick, S., and De Camilli, P. (1998). Synaptotjanin family members are implicated in endocytic membrane traffic in yeast. *J. Cell Sci.* 111, 3347–3356.
- Singer-Kruger, B., Stenmark, H., Dusterhoft, A., Philippsen, P., Yoo, J.S., Gallwitz, D., and Zerial, M. (1994). Role of three rab5-like GTPases, Ypt51p, Ypt52p, and Ypt53p, in the endocytic and vacuolar protein sorting pathways of yeast. *J. Cell Biol.* 125, 283–298.
- Singer-Kruger, B., Stenmark, H., and Zerial, M. (1995). Yeast Ypt51p and mammalian Rab5: counterparts with similar function in the early endocytic pathway. *J. Cell Sci.* 108, 3509–3521.

- Tang, H., Munn, A., and Cai, M. (1997). EH domain proteins Pan1p and End3p are components of a complex that plays a dual role in organization of the cortical actin cytoskeleton and endocytosis in *Saccharomyces cerevisiae*. *Mol. Biol. Cell* 17, 4294–4204.
- van Genderen, I., van Meer, G., Slot, J., Geuze, H., and Voorhout, W. (1991). Subcellular localization of Forssman glycolipid in epithelial MDCK cells by immuno-electron microscopy after freeze-substitution. *J. Cell Biol.* 115, 1009–1019.
- van Tuinen, E., and Riezman, H. (1987). Immunolocalization of glyceraldehyde-3-phosphate dehydrogenase, hexokinase, and carboxypeptidase Y in yeast cells at the ultrastructural level. *J. Histochem. Cytochem.* 35, 327–333.
- Vida, T.A., Huyer, G., and Emr, S.D. (1993). Yeast vacuolar proenzymes are sorted in the late Golgi complex and transported to the vacuole via a prevacuolar endosome-like compartment. *J. Cell Biol.* 121, 1245–1256.
- Waddle, E., Karpova, T., Waterston, R., and Cooper, J. (1996). Movement of cortical actin patches in yeast. *J. Cell Biol.* 132, 861–870.
- Wendland, B., and Emr, S. (1998). Pan1p, yeast eps15, functions as multivalent adaptor that coordinates protein-protein interactions essential for endocytosis. *J. Cell Biol.* 141, 71–84.
- Wendland, B., McCaffery, J.M., Xiao, Q., and Emr, S.D. (1996). A novel fluorescence-activated cell sorter-based screen for yeast endocytosis mutants identifies a yeast homologue of mammalian eps15. *J. Cell Biol.* 135, 1485–1500.
- Wesp, A., Hicke, L., Palecek, J., Lombardi, R., Aust, T., Munn, A., and Riezman, H. (1997). End4p/S1a2p interacts with actin-associated proteins for endocytosis in *Saccharomyces cerevisiae*. *Mol. Biol. Cell* 8, 2291–2306.
- Wright, R., and Rine, J. (1989). Transmission electron microscopy and immunocytochemical studies of yeast: analysis of HMG-CoA reductase overproduction by electron microscopy. *Methods Cell Biol.* 31, 473–512.
- Zerial, M., and Stenmark, H. (1993). Rab GTPases in vesicular transport. *Curr. Opin. Cell Biol.* 5, 613–620.